BBA - Molecular Basis of Disease 1865 (2019) 2180–2188

Contents lists available at ScienceDirect

BBA - Molecular Basis of Disease

journal homepage: www.elsevier.com/locate/bbadis

H^+-dependent inorganic phosphate transporter in breast cancer cells: Possible functions in the tumor microenvironment☆

Marco Antonio Lacerda-Abreu[a,b], Thais Russo-Abrahão[a,b], Daniela Cosentino-Gomes[a,b], Michelle Tanny Cunha Nascimento[a,b], Luiz Fernando Carvalho-Kelly[a,b], Tainá Gomes[a], Mariana Figueiredo Rodrigues[a], Sandra König[c], Franklin David Rumjanek[a], Robson Q. Monteiro[a], José Roberto Meyer-Fernandes[a,b,*]

[a] Instituto de Bioquímica Médica Leopoldo de Meis, Universidade Federal do Rio de Janeiro, RJ, Brazil
[b] Instituto Nacional de Ciência e Tecnologia em Biologia Estrutural e Bioimagem, Rio de Janeiro, RJ, Brazil
[c] Instituto de Ciência Biomédicas, Universidade Federal do Rio de Janeiro, RJ, Brazil

ARTICLE INFO

Keywords:
Inorganic phosphate
H^+-dependent Pi transport
Breast cancer
MDA-MB-231

ABSTRACT

Tumor microenvironment has a high concentration of inorganic phosphate (Pi), which is actually a marker for tumor progression. Regarding Pi another class of transporter has been recently studied, an H^+-dependent Pi transporter, that is stimulated at acidic pH in Caco2BBE human intestinal cells. In this study, we characterized the H^+-dependent Pi transport in breast cancer cell (MDA-MB-231) and around the cancer tissue. MDA-MB-231 cell line presented higher levels of H^+-dependent Pi transport as compared to other breast cell lines, such as MCF-10A, MCF-7 and T47-D. The Pi transport was linear as a function of time and exhibited a Michaelis-Menten kinetic of $K_m = 1.387 \pm 0.1674$ mM Pi and $V_{max} = 198.6 \pm 10.23$ Pi $\times h^{-1} \times$ mg protein^{-1} hence reflecting a low affinity Pi transport. H^+-dependent Pi uptake was higher at acidic pH. FCCP, Bafilomycin A1 and SCH28080, which deregulate the intracellular levels of protons, inhibited the H^+-dependent Pi transport. No effect on pHi was observed in the absence of inorganic phosphate. PAA, an H^+-dependent Pi transport inhibitor, reduced the Pi transport activity, cell proliferation, adhesion, and migration. Arsenate, a structural analog of Pi, inhibited the Pi transport. At high Pi conditions, the H^+-dependent Pi transport was five-fold higher than the Na^+-dependent Pi transport, thus reflecting a low affinity Pi transport. The occurrence of an H^+-dependent Pi transporter in tumor cells may endow them with an alternative path for Pi uptake in situations in which Na^+-dependent Pi transport is saturated within the tumor microenvironment, thus regulating the energetically expensive tumor processes.

1. Introduction

In many, if not all living organisms inorganic phosphate (Pi) is obtained from the diet in three anionic forms (H_2PO_4, HPO_4 or H_3PO_4). Pi is essential for several biochemical reactions such as the kinase/phosphatase signaling, formation of ATP, biosynthesis of lipids, carbohydrates and nucleic acids [1,2].

In healthy mammals, the extracellular [Pi] is maintained at relatively narrow range concentrations, between 0.7 and 1.55 mM [3,4]. Pi is absorbed by cells through Pi transporters. It has been established that Pi is transported mainly via Na/Pi cotransporters, consisting of two large carrier families: SLC20 (which includes PiT-1, encoded by SLC20A1 gene, PiT-2, encoded by SLC20A2 gene), and SLC34 (which includes NaPi-IIa, encoded by SLC34A1, NaPi-IIb, encoded by SLC34A2 and NaPi-IIc, encoded by SLC34A3) [5–9].

Although Na^+-dependent Pi transporters have been investigated in detail, studies on another class of H^+-dependent Pi transporters stimulated at acidic pH are emerging [10–14]. Shirazi-Beeche and coworkers observed a Pi transport insensitive to phosphonoformic acid (PFA,) a specific inhibitor of Na^+-dependent Pi transport in oocytes [10].

H^+-dependent Pi transporter has been thoroughly investigated in osteoclasts-like cells demonstrating that the intracellular pH decreased with the addition of Pi and that H^+-dependent Pi transport was

☆ This work is dedicated to Ottilia Rodrigues Affonso Mitidieri on her 92th birthday.

* Corresponding author at: Laboratório de Bioquímica Celular, Instituto de Bioquímica Médica Leopoldo De Meis, Universidade Federal do Rio de Janeiro, CCS, Cidade Universitária, Rio de Janeiro, RJ 21941-590, Brazil.
E-mail address: meyer@bioqmed.ufrj.br (J.R. Meyer-Fernandes).

https://doi.org/10.1016/j.bbadis.2019.04.015
Received 23 February 2018; Received in revised form 20 December 2018; Accepted 6 January 2019
Available online 26 April 2019

regulated by a V-H^+-ATPase, suggesting that it could be involved in the removal of intracellular protons and acidification of the extracellular milieu [12].

Studies on human intestinal cells (Caco2BBE) showed that the phosphate transport is uniquely Na^+-independent, displaying more than one kinetic component, and at least one of them being an H^+-dependent process [13]. When these cells were incubated with high levels of phosphate (4 mM), an independent uptake of Na^+ was stimulated [13].

Compared to normal cells it has been established that tumor cells have a higher demand for phosphate due to their rapid growth rates. This is in accordance with the Growth Rate Hypothesis (GRH) [15–17]. Indeed the intracellular levels of Pi in tumor cells have been shown to range from 2 to 7 mM [15,18,19].

For instance, the difference between Pi in the tumor microenvironment 1.8 ± 0.2 mM Pi, and that of normal mammary gland, 0.84 ± 0.07 mM Pi was considered to be a marker for tumor breast cancer cells lines. The markers are classified by expression patterns of oncogenic receptors, such as MCF-7 and T47-D cells (Luminal A, ER+, PR+ and HER-) or MDA-MB-231 (triple-negative overexpression: ER-, PR- and HER-) [15,20–22]. Studies in vitro with breast cancer cells, such as MCF-7, T47-D and MDA-MB-231, have demonstrated that MDA-MB-231 exhibits an increased migratory capacity when compared to MCF-7 and T47-D [23]. It has also been shown that the migration of MDA-MB-231 cells was enhanced in the presence of high Pi concentrations (3 or 5 mM), this being a hallmark of the metastatic process [24]. SLC34A2 gene expression is significantly increased in breast cancer compared to adjacent normal breast tissues. Overexpression of SLC34A2 gene was similar to that of CA125, one of the well-known cancer biomarkers. This observation suggests that SLC34A2 may be a novel marker for diagnosis and potentially a target for the therapy of breast cancer [25]. Recently, we measured the kinetic parameters of sodium-dependent Pi transport in the aggressive human breast cancer cell lines. The Pi transport level was found to be higher in cells with greater metastatic potential such as MDA-MB-231. In addition, inhibition of Na^+-dependent Pi transport in those cells reduced tumor cell migration and adhesion [26] yet another indication that the metastatic phenotype might be functionally associated to Pi transport.

As an extension of these previous observations in the present work we aimed at determining the inorganic phosphate transport in the presence of high levels of Pi (1 mM) in different human breast cell lines including the non-tumorigenic MCF-10A and the malignant MCF-7, T47-D and MDA-MB-231. We further characterize biochemically the H^+-dependent inorganic phosphate transport on MDA-MB-231 cells seeking a possible association between the H^+-dependent Pi transport and cell adhesion and migration in this tumor cell line.

2. Materials and methods

2.1. Materials

Reagents were purchased from E. Merck (Darmstadt, Germany) and Sigma Chemical Co. (St. Louis, MO, USA). All solutions were prepared with Milli-Q water (Millipore Corp., Bedford, MA, USA). The inorganic radioactive phosphate (^{32}Pi) was supplied by the Nuclear and Energy Research Institute (IPEN).

2.2. Cell culture

Human breast non-tumorigenic epithelial cell line, MCF-10A, were grown at 37 °C in a humidified atmosphere of 5% CO_2 in Dulbecco's Modified Eagle Medium/Nutrient Mixture F-12 (DMEM/F-12), 10% fetal bovine serum (FBS), 10 μg/mL insulin (Sigma–Aldrich, St. Louis, MO), 20 ng/mL Epidermal Growth Factor (EGF) (Sigma–Aldrich, St. Louis, MO), 0.5 μg/mL hydrocortisone, pH 7.4 (Sigma–Aldrich, St. Louis, MO), 100 U/mL penicillin and streptomycin (Thermo Fisher, Brazil). MCF-10A cells, genotyped yielding a profile that confirms their identity by comparing it to data of ATCC, DSMZ, CLIMA and ICLAC, was kindly supplied by Jerson Lima da Silva from the Instituto de Bioquímica Médica Leopoldo De Meis, UFRJ, Rio de Janeiro, Brazil and. Breast cancer cell lines (MDA-MB-231, T47D and MCF-7) were grown at 37 °C in a humidified atmosphere of 5% CO_2 in Iscoves Modified Dulbecco's Medium (IMDM-LCG Biotechnology, Brazil) supplemented with sodium bicarbonate, 10% fetal bovine serum (FBS) (Cripion Biotechnology, Brazil), 100 U/mL penicillin and streptomycin (Thermo Fisher, Brazil). IMDM contains 1 mM Pi and added NaH_2PO_4, pH was adjusted to 7.4 with HCl (Sigma–Aldrich, St. Louis, MO).

Prior to the experiments, breast cancer cell lines were washed twice with a free-phosphate buffer solution containing 116 mM NaCl, 5.4 mM KCl, 5.5 mM glucose, 0.8 mM $MgCl_2$ and 50 mM HEPES (pH 7.2). Cells used for experimental conditions indicated as H^+-dependent (or Na^+-independent) were washed with buffer solution containing 116 mM choline chloride, 5.4 mM KCl, 5.5 mM glucose, 0.8 mM $MgCl_2$ and 50 mM HEPES (pH 7.2). Adherent cells were dissociated after incubation at 37 °C, 5% CO_2 with a trypsin solution (2.5 g/L, pH 7.2, 0.05 mL/cm^2), and the number was estimated by counting in a Neubauer chamber. Protein concentration was measured using the Bradford method [27].

2.3. Pi transport assay

MCF-10A, MDA-MB-231, T-47D and MCF-7 (5×10^4 cells per well) were incubated at 37 °C, 5% CO_2 atmosphere, for 40 min in a reaction mixture (0.5 mL) containing 116 mM NaCl or choline chloride, 5.4 mM KCl, 5.5 mM glucose, 50 mM HEPES (pH 7.2), 0.8 mM $MgCl_2$, 1 mM KH_2PO_4 and 2.5 μCi/nmol ^{32}Pi. In parallel, the transport of Pi was carried out at 4 °C as a control (blank values) [28]. Reactions were stopped and cells was washed with 0.5 mL of an ice-cold phosphate buffer saline (PBS) (pH 7.2) and cells were lysed with 0.5 mL SDS 0.1%. These internalized Pi released by cell lysis was transferred to a filter paper which was then immersed in scintillation liquid [26,28].

To determine Pi H^+-dependent (or Na^+-independent) transport values, NaCl was replaced by choline chloride. In order to determine Pi Na^+-dependent activity, transport values of Pi in the presence of NaCl were subtracted from the values of transport of Pi in the presence of choline chloride, thus deriving the NaCl stimulated fraction.

To measure substrate affinity (K_m) and maximum rate (V_{max}) of the Pi transporter concentrations of Pi ranging from 0 to 5 mM Pi were used. Bafilomycin A1 (100 nM), the vacuolar ATPase inhibitor, valinomycin (100 μM), the K+ ionophore, FCCP (10 nM), the H^+ ionophore, and monensin (100 μM), the Na^+ ionophore, were tested. The H^+, K^+-ATPase inhibitor, SCH28080 (100 μM), 4,4′-Diisothiocyano-2,2′-stilbenedisulfonic acid (DIDS), an anion exchange inhibitor and the Pi transport inhibitors, phosphonoformic acid (PFA-5 mM), phosphonoacetic acid (PAA-1 mM) and arsenate (1 mM) were also tested. Vehicles were: 1% DMSO (bafilomycin A1, valinomycin, furosemide and SCH28080), ethanol 1% (monensin), and water (DIDS, PFA, PAA, arsenate) were used in control conditions. At 1% of these vehicles, the values obtained for ^{32}Pi uptake were the same as those obtained with water. The viability of MDA-MB-231 was tested using the CellTiter 96® AQueous One Solution Cell Proliferation Assay (MTS) (Promega, USA), according to the manufacturer's instructions.

2.4. Real-time PCR analysis

Total RNA from MDA-MB-231 cells was purified from TRIzol Reagent (Invitrogen, Thermo Fisher Scientific, Massachusetts, USA) as described in the manufacturer's manual. After treatment of RNA with DNase I, a firs-strand synthesis kit (Invitrogen) was used to generate the full-length cDNA from 1 μg of total RNA. qPCR was performed on StepONE Plus Real Time PCR System (Applied Biosystems, Massachusetts, USA) using a FastStart Master SYBR Green I kit (from

Roche, Mannheim, Germany). The expression data of the NaPi-IIb gene (sense primer: 5′-CCCAGCTTATAGTGGAGAGCTTC-3′; antisense prime: 5′-GCACCAAATCTTGACAAGACTCTTG-3′) were normalized to an endogenous reference (β-actin, sense primer: 5′-TGACGTGGACATCCGC AAAG-3′; antisense primer: 5′-CTGGAAGGTGGACAGCGAGG-3′) as previously described [29] and according to the manufacturer's instructions.

2.5. Proliferation assay

MDA-MB-231 cells (1×10^4 cells per well) were seeded in 24-well plates. After 12 h, 1 mM of PAA was added, and cells were incubated for different times at 37 °C in 5% CO_2 atmosphere. After the respective incubation time (0–60 h), cells were washed twice with PBS, trypsinized and quantified using a Neubauer chamber.

2.6. Adhesion assay

96-Well culture plates were pre-coated with 32 μg/mL ECM gel (rat sarcoma) diluted in PBS. Then 100 μL per well were added for 12 h at 4 °C. In order to block non-specific, background binding sites of the wells, they were blocked with 1 mg/ml BSA, diluted in PBS for 2 h at room temperature. 100 μL of MDA-MB-231 cells suspended in serum-free medium at 2.5×10^4 cells/well were added to each well coated with ECM gel in the absence or presence of 1 mM PAA and maintained at 37 °C, 5% CO_2, for 12 h. After incubation, non-adherent cells were carefully removed by washing twice with PBS and fixed with 3% paraformaldehyde for 10 min. Fixed cells were then washed with PBS twice, stained with 100 μL of 0.5% crystal violet, for 5 min and washed further (2×) with PBS. The washed cells were lysed with 100 μL acetic acid (1% in ethanol) and stained with crystal violet. Cell lysates were read spectrophotometrically at 570 nm. Results were expressed as control percentage [30].

2.7. Migration assay

24 well plates Corning© Transwell© were used for migration assays through the permeable supports with 6.5 mm insert, and polycarbonate membrane pore with 8.0 μm. MDA-MB-231 cells (5×10^4 cells/well) were suspended in serum-free medium and added to the upper chamber in the absence or presence of 1 mM PAA, maintained at 37 °C, 5% CO_2, for 24 h. After incubation, the non-adherent cells were removed after two washes with PBS, and subsequently, cells were trypsinized and quantified using Neubauer chamber.

2.8. Optical quantification of intracellular pH

To analyze changes in intracellular pH (pHi) after Pi influx, MDA-MB-231 cells (1×10^5 cells per well) were washed three times in buffer solution containing 116 mM NaCl, 5.4 mM KCl, 5.5 mM glucose, 0.8 mM $MgCl_2$ and 50 mM HEPES (pH 7.2) and incubated for 30 min with 6 μM BCECF-AM (Thermo Fisher). Cells were washed to remove the excess extracellular BCECF-AM and plated in 96 well plates with same buffer solution. Time 0 measurements were performed just before the addition of 1 mM KH_2PO_4. Intracellular pH changes were quantified using a VICTOR multiplate reader with excitation and emission wavelengths of 500 and 550 nm, respectively, according to manufacturer's instructions. pHi was measured at 2-minute intervals after addition of 1 mM KH_2PO_4. The ratio of fluorescence to excitation emission was converted to pH values using high-K nigericin method [31].

2.9. Immunofluorescence imaging

MDA-MB 231 cells were treated or not with 1 mM PAA for 24 h. Cells were then rinsed two times with PBS and fixed with 4% paraformaldehyde for 24 h, permeabilized with 0.1% Triton X-100 in PBS for 5 min and unspecific sites were blocked in 5% PBS-BSA for 2 h. Samples were then incubated at 4 °C overnight with mouse-anti-vimentin (1:100; DAKO clone V9) or mouse-anti-E-cadherin (1:100; BD610182) antibodies. After extensive wash, samples were stained with goat-anti-mouse IgG (H + L) secondary antibody conjugated with Alexa Fluor®–594 (1:500; Molecular Probes A11032) for 1 h at room temperature and extensively washed. Slides were mounted using ProLong® Gold Antifade Mountant with DAPI. Images were taken using confocal high-resolution LSM 710 equipped with Elyra PS.1 system and sCMOS-pco camera (ZEISS). Images were analyzed by ZEN lite blue edition software (ZEISS). Fluorescence intensities were quantified by Image J software as the pixel of red-staining intensity per cell (from 10 cells for each experimental condition). Statistical significance of the quantification was analyzed applying unpaired *t*-test.

2.10. Statistical analysis

In all cases, at least three independent experiments were performed in triplicate. The values presented in all experiments represent the mean ± SE. The kinetic parameters (apparent values of K_m and Vmax) were calculated using the non-linear regression analysis of data for Michaelis-Menten equation. Linear regression analysis of Lineweaver-Burk plots was also determined. Differences were considered significant at $p < 0.05$ by One-Way analysis of variance (ANOVA), using Turkey's multiple comparisons test, unless otherwise specified in the figure legends. All statistical analyzes were performed with GraphPad Prism 6.0 software (GraphPad Software, San Diego, USA).

3. Results

3.1. Pi transport in different breast cancer cells lineages

One non-tumorigenic cell line (MCF-10A) and three breast cancer cell lines were used to measure the level of H^+-dependent (or Na^+-independent) Pi transport with 1 mM Pi: MCF-7, T47D (both classified as luminal A) and MDA-MB-231 (classified as triple negative) [21,22]. MCF-10 presented H^+-dependent Pi transport (Fig. 1). It is important to note that, in the presence of 1 mM Pi, the Na^+-dependent Pi transport is saturated. Cell lines classified as luminal A (MCF-7 and T47-D) also presented H^+-dependent Pi transport levels without significant differences among them. However, MDA-MB-231 line displayed a higher level of H^+-dependent Pi transport as compared to MCF-10, MCF-7 and T47-D (Fig. 1).

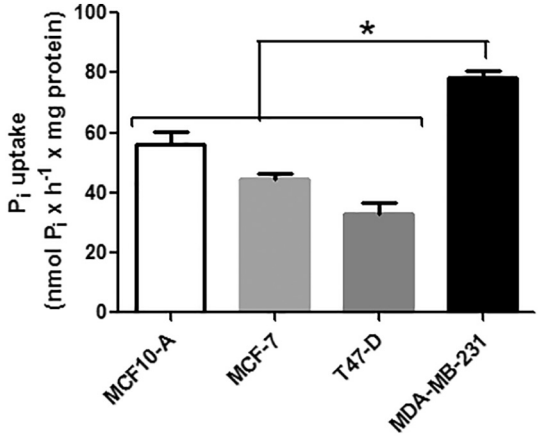

Fig. 1. Comparative rates of ^{32}Pi influx in breast cell lines. Intact MCF-10A, MCF-7, T47-D or MDA-MB-231 cells (5×10^4 cells/well = 1.45 mg protein/mL) were incubated at 37 °C in a reaction mixture containing 116 mM choline cloride, 5.5 mM Glucose, 5.4 KCl, 10 mM HEPES, 0.8 mM $MgCl_2$, 1 mM KH_2PO_4 and 2.5 μCi/nmol ^{32}Pi. The results are the means ± SE of at least 3 experiments, with different cell suspensions.

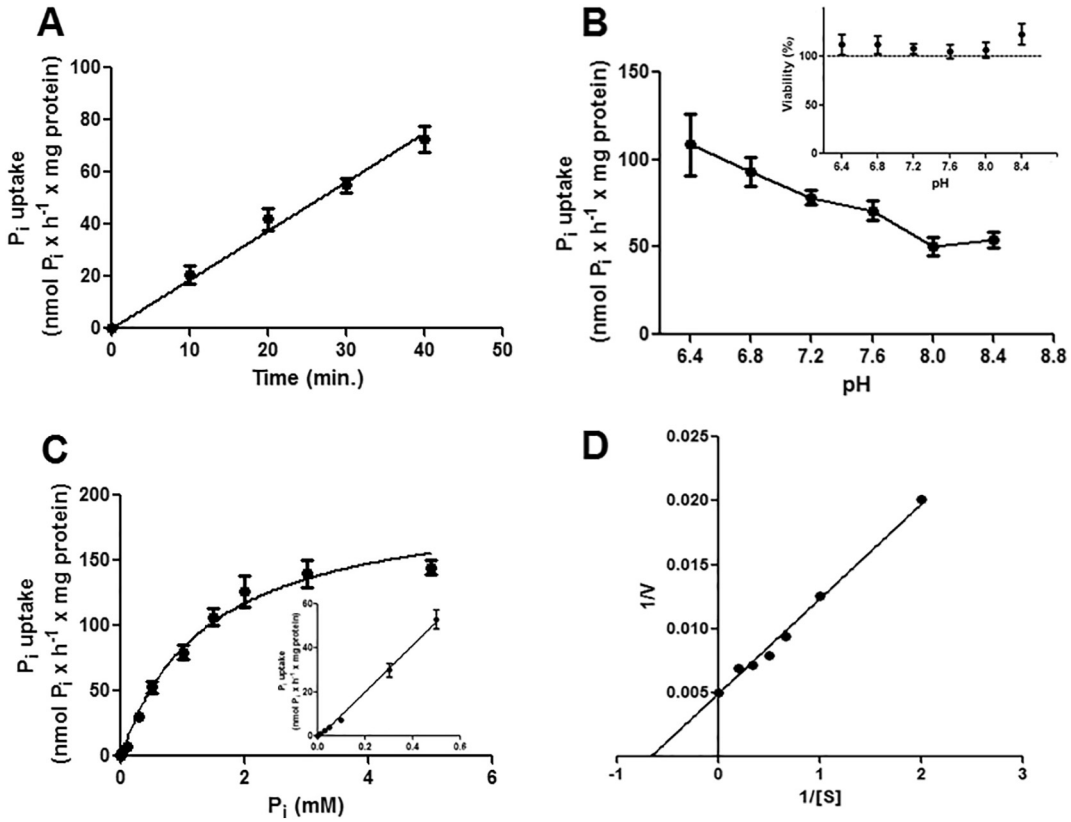

Fig. 2. Kinetic parameters of H^+-dependent ^{32}Pi influx of MDA-MB-231 cells. Intact cells (5×10^4 cells/well = 1.45 mg protein/mL) were incubated at 37 °C in a reaction mixture as described in Fig. 1 at various times (A), pH ranging from 6.4 to 9.2 using 10 mM HEPES, 15 mM Tris, 15 mM MES (B), increasing concentrations of KH_2PO_4 (0–5 mM) (C), Lineweaver-Burk plot for Pi concentrations between 0.5 and 5 mM Pi (D). In these pH ranges, the cells remained viable throughout the experiment according to CellTiter 96®AQueous One Solution Cell Proliferation Assay (MTS) (C inset). The results are the means ± SE of at least 3 experiments, with different cell suspensions.

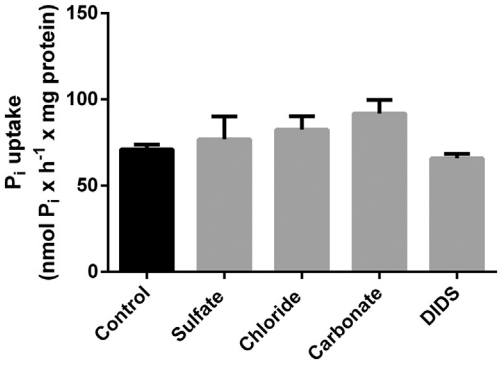

Fig. 3. Effect of anions on H^+-dependent ^{32}Pi influx of MDA-MB-231 cells. Intact cells (5×10^4 cells/well = 1.45 mg protein/mL) were incubated for 40 min at 37 °C in a reaction mixture as described in Fig. 1 and anions or inhibitor indicated in the horizontal axis: magnesium sulfate (10 mM), magnesium chloride (10 mM), magnesium bicarbonate (10 mM) and DIDS (1 mM). In the presence of these inhibitors at their respective concentrations, cells remained viable throughout the experiment. Results are the means ± SE of at least 3 experiments, with different cell suspensions.

3.2. H^+-dependent Pi transport of MDA-MB-231 cells

Next we biochemically characterized the H^+-dependent inorganic phosphate transport in MDA-MB-231. H^+-dependent Pi transport tests were carried out at different times from 0 to 40 min. We could observe linearity of the transport as a function of time for up to 40 min (Fig. 2A). Because longer times could lead to saturation of Pi transport, we used 40 min as the standard time for Pi capture in Pi transport assays throughout the work.

H^+-dependent inorganic phosphate transport assays were carried out at different pH ranges (6.4 to 9.2). The result in Fig. 2B shows that the higher Pi uptake occurred at more acidic pH. In all pH ranges performed, cell viability in MDA-MB-231 was not affected (Fig. 2B *inset*).

Assays in the presence of different Pi concentrations were carried out in MDA-MB-231 cells. A Michaelis-Menten kinetic profile for the H^+-dependent transport of Pi was observed in the presence of increasing concentrations of inorganic phosphate from 0 to 5 mM until saturation was reached (Fig. 2C). This yielded a value of $K_m = 1.387 \pm 0.1674$ mM Pi and $V_{max} = 198.6 \pm 10.23$ Pi $\times$ $h^{-1} \times$ mg $protein^{-1}$. A double reciprocal plot is shown in Fig. 2D. Compared to the data presented previously for Na^+-dependent Pi transport [26], the carrier analyzed here exhibits low affinity for inorganic phosphate.

3.3. Influence of anions to H^+-dependent Pi transport

Inorganic phosphate is a negatively charged compound, chemically classified as an anion. Several studies have described a nonspecific anion transporter in Caco2BBE cells [13]. To investigate whether the H^+-dependent inorganic phosphate transport would indeed be an anion carrier, magnesium sulfate (10 mM), magnesium chloride (10 mM) and magnesium bicarbonate (10 mM) were tested in H^+-dependent Pi transport [13]. No effects of these anions were observed (Fig. 3). In addition, the classical inhibitor of anion transporters (4,4′-Diisothiocyano-2,2′-stilbenedisulfonic acid – DIDS) [13] had no significant effect on the H^+-dependent Pi transport at 1 mM concentration (Fig. 3).

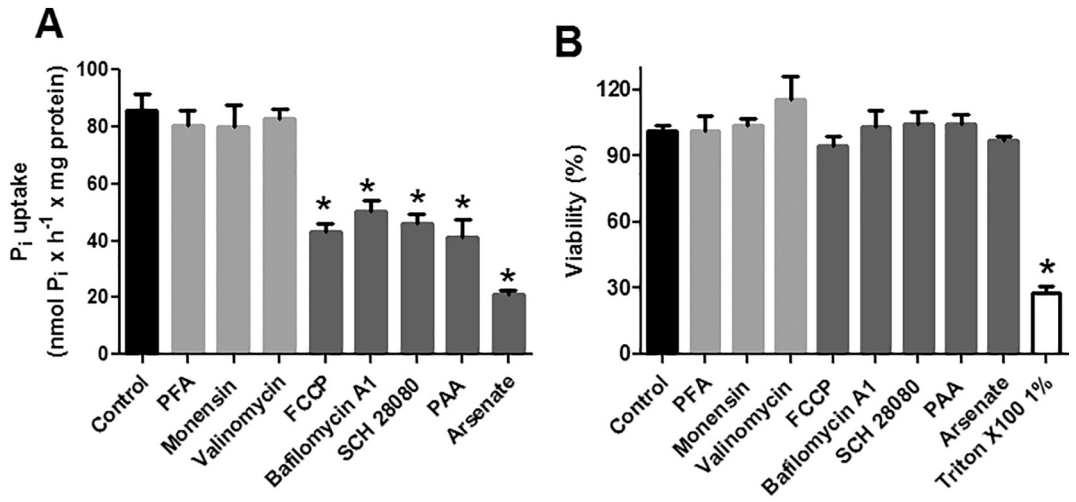

Fig. 4. Effect of ion influx on H^+-dependent ^{32}Pi uptake of MDA-MB-231 cells. Intact cells (5×10^4 cells/well = 1.45 mg protein/mL) were incubated for 40 min at 37 °C in a reaction mixture as described in Fig. 1 and the inhibitors indicated in the abscissa: PFA (5 mM), monensin (100 μM), FCCP (10 μM), bafilomycin A1 (100 nM), SCH28080 (100 μM), valinomycin (100 μM), PAA (1 mM), arsenate (1 mM) (A). In the presence of these inhibitors at their respective concentrations, cells remained viable throughout the experiment according to CellTiter 96®AQueous One Solution Cell Proliferation Assay (MTS) (B). Results are the means ± SE of at least 3 experiments, with different cell suspensions.

3.4. Influence of ion influx inhibitors on H^+-dependent Pi transport

In order to verify the importance of the ion influx for the H^+-dependent Pi transport, assays were performed in the presence of different ion transport modulators. Those were PFA (phosphonoformic acid), an inhibitor of the Na^+-dependent Pi transporter; Monensin, a Na^+ ionophore; Valinomycin, a K^+ ionophore, and FCCP, an H^+ ionophore. In addition, inhibitors of the vacuolar H^+-ATPase, Bafilomycin A1, an inhibitor of H^+, K^+-ATPase, SCH28080, a Pi transport inhibitor, PAA, and arsenate, a structural analog of Pi, were also tested. Only FCCP, Bafilomycin A1 and SCH28080, which deregulate the levels of intracellular protons, as well as PAA and arsenate inhibited H^+-dependent Pi transport (Fig. 4A). In all conditions performed, MDA-MB-231 cell viability was not affected (Fig. 4B).

3.5. Proton participation in Na^+-independent Pi transport

To verify the hypothesis that Na^+-independent Pi transport is an H^+-dependent Pi transporter, optical quantification of intracellular pH was initially carried out using permeabilized MDA-MB-231 cells at pH values ranging from 5.5 to 8.5. The intracellular pH (pHi) of MDA-MB-231 cells was measured at various times in the presence or absence of inorganic phosphate (1 mM). The results in Fig. 5 show that addition of inorganic phosphate lowered pHi. No effect on pHi was observed in the absence of inorganic phosphate.

3.6. Effect of PAA on Pi transport, cell proliferation, adhesion and migration phenotype

It has been reported that phosphonoacetic acid (PAA) is a potent inhibitor of H^+-dependent Pi transport [13]. In Fig. 6A we show the effect of increasing concentrations of PAA on H^+-dependent Pi transport. Based on that, 1 mM of PAA was tested for several parameters relevant to tumor cell behavior. MDA-MB-231 cell proliferation was evaluated over 60 h. We found that proliferation was reduced by approximately 80% in the presence of PAA compared to controls (Fig. 6B). PAA was also tested in adhesion and migration assays. The results in Fig. 6C and D show that 1 mM PAA reduced both parameters by approximately 40%. In addition, migrating cells displayed higher Pi transport activity than non-migrating cells, as shows in Fig. 6E. In contrast, there was no difference between these two conditions when Pi

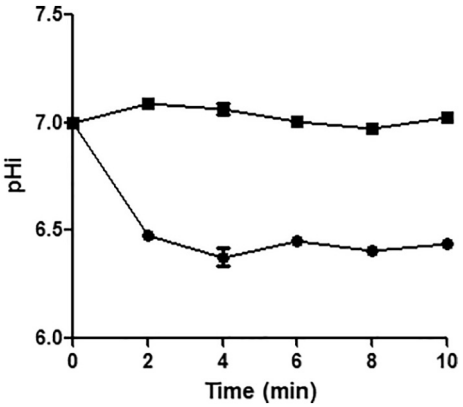

Fig. 5. Influence of inorganic phosphate on intracellular pH as a function of time in MDA-MB-231. A) Intact cells (5×10^4 cells/well = 1.45 mg protein/mL) were washed with a reaction mixture containing 116 mM choline chloride, 5.5 mM Glucose, 10 mM HEPES, 0.8 mM $MgCl_2$. 1 mM KH_2PO_4 (closed circle) or water (closed square) were added. The intracellular pH (pHi) was quantified each 2 min interval for 10 min total time by optical quantification of the intracellular pH. Results are the means ± SE of at least 3 experiments, with different cell suspensions.

transport activity was measured at 100 μM Pi, a suitable condition for high-affinity Na^+-Pi-transport (Fig. 6F).

We also analyzed the marker proteins associated with the Epithelial-Mesenchymal Transition (EMT) (E-cadherin and vimentin) and migration capacity of MDA-MB-231 cells grown in the presence or absence of PAA by immunofluorescence. While control cells presented low expression of E-cadherin (Fig. 7A) and high expression of vimentin (Fig. 7F), cells grown in the presence of PAA for 24 h present induced expression of E-cadherin (Fig. 7B), suggesting an inverted pattern of markers expression. Quantification of the fluorescence intensity confirmed that PAA significantly increases E-cadherin expression (Fig. 7E). These observations strongly suggest that, when Pi transport is inhibited, MDA-MB-231 cells tend to revert from mesenchymal to epithelial features.

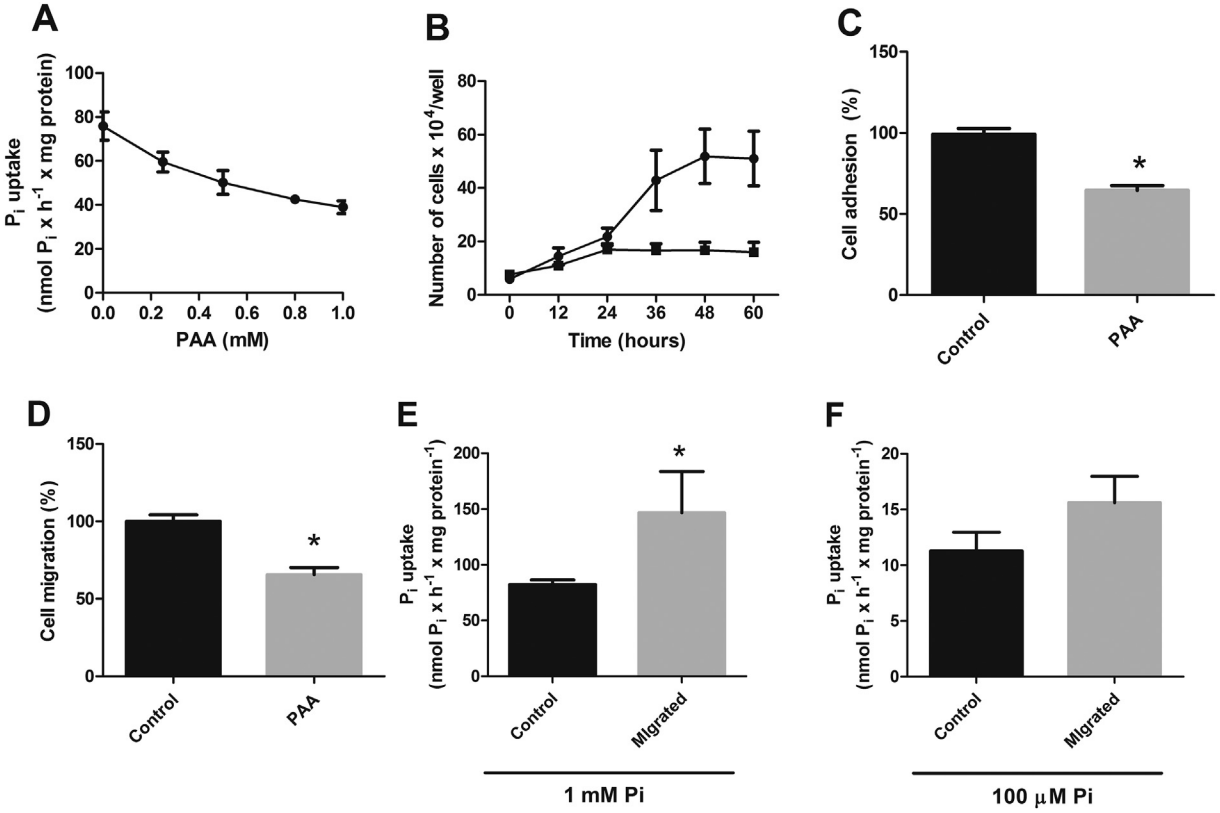

Fig. 6. Effect of PAA on ^{32}Pi influx, proliferation, adhesion and cell migration phenotype in MDA-MB-231. Intact cells (5×10^4 cells/well = 1.45 mg protein/mL) were incubated for 40 min at 37 °C in a reaction mixture as described in Fig. 1 in the presence of increasing concentrations of PAA, where cells remained viable throughout the experiment (A). MDA-MB-231 (1×10^4 cells/well) were maintained in 1 mM PAA were quantified at an initial interval of 6 or 12 h up to 60 h using Neubauer camera (B). Cell adhesion were done with MDA-MB-231 cells (5×10^4 cells/well) pretreated for 40 min in the presence or absence of PAA (1 mM) (C). Cell migration were done with MDA-MB-231 cells (5×10^4 cells/well) pretreated for 40 min in the presence or absence of PAA (1 mM) (D). Pi transport was measured, in the same condition described previously, in non-migrated (control) or migrated cells in the presence of 1 mM Pi (E) or 100 µM Pi (F). Results are the means ± SE of at least 3 experiments, with different cell suspensions.

3.7. Effect of high phosphate concentration and PFA in growth medium on Pi transport

In mammary gland tumors of mice, a high concentration of Pi in the tumor microenvironment (~2 mM Pi), compared to that in the normal mammary gland (approximately 1 mM Pi) was identified [20]. MDA-MB-231 cells were maintained at different Pi concentrations (1 or 2 mM Pi) and in the presence of PFA (5 mM) in the growth medium for 24 h. As shown in Fig. 8A, NaPi-IIb expression was significantly decreased at 2 mM Pi as well at 5 mM PFA.

Parallel experiments with MDA-MB-231 cells in the same conditions were carried out. Cells were washed in a Pi free solution and 100 µM Pi was added thereafter to analyze the Pi transport. Na^+-dependent Pi transport was abolished at 5 mM PFA and significantly decreased in the presence of 2 mM Pi (Fig. 8B). However, the H^+-dependent Pi transport at 2 mM or 5 mM Pi was 5 fold higher than the Na^+-dependent Pi transport (Fig. 8B).

4. Discussion

Recently, our group characterized the high-affinity Na^+-dependent Pi transporter in MDA-MB-231 cells [26]. Throughout that work, low Pi concentrations (100 µM Pi) were used for the Pi transport assays. In the present work, 1 mM Pi was used in Pi transport assays in order to characterize an H^+-dependent Pi transporter that responds to high Pi concentrations. Based on the results shown in Fig. 1, we suggest that the enhanced H^+-dependent Pi transport may contribute to greater migratory capacity [23]. In this situation the excess Pi transport would be in keeping with a greater demand for Pi in connection with tumor cell energy metabolism. We propose then that there is another kinetic component responsive to high Pi concentrations in breast cancer cells, which was analyzed in detail in the present work.

Our results showed that the influence of sodium and potassium could be discarded based on experiments in which valinomycin, monensin and PFA were used (Fig. 4A). Furthermore, H^+-dependent Pi transport was linear for up to 40 min (Fig. 2A) and exhibited a Michaelis-Menten kinetics displaying low affinity for inorganic phosphate (Fig. 2C and D). This result is compatible with that of osteoclast-like cells, in which the transport system has a K_m to Pi of 7.5 mM (low affinity component) and 0.35 mM (high affinity component) [12]. Presumably this low affinity Pi transport becomes operative when the levels of Pi in tumor microenvironment rise to 2 mM thus contributing to scavenge the excess Pi when the Na^+-dependent transporter is saturated, with K_m = 0.08 mM Pi and V_{max} = 71.67 ± 3 nmol × h^{-1} × $(mg\ protein)^{-1}$ [26].

Candeal and coworkers (2014) characterized an H^+-dependent Pi transport in human intestinal cells (Caco2BBE) [13] and observed that the Pi transport was influenced by anions, suggesting that Pi could be taken up along with others anions. In our study, no effect was observed when anions and anion-carrier inhibitor (DIDS) were tested on H^+-dependent Pi transport of MDA-MB-231 (Fig. 3). These results suggested that Pi uptake by breast cancer cells did not involve an anion carrier.

Extracellular pH can be acidified by the secretion of lactate and H^+ catalyzed by monocarboxylate transporter 4 (MCT) in cancer cells. This may be relevant to our observations in the sense that a greater Pi

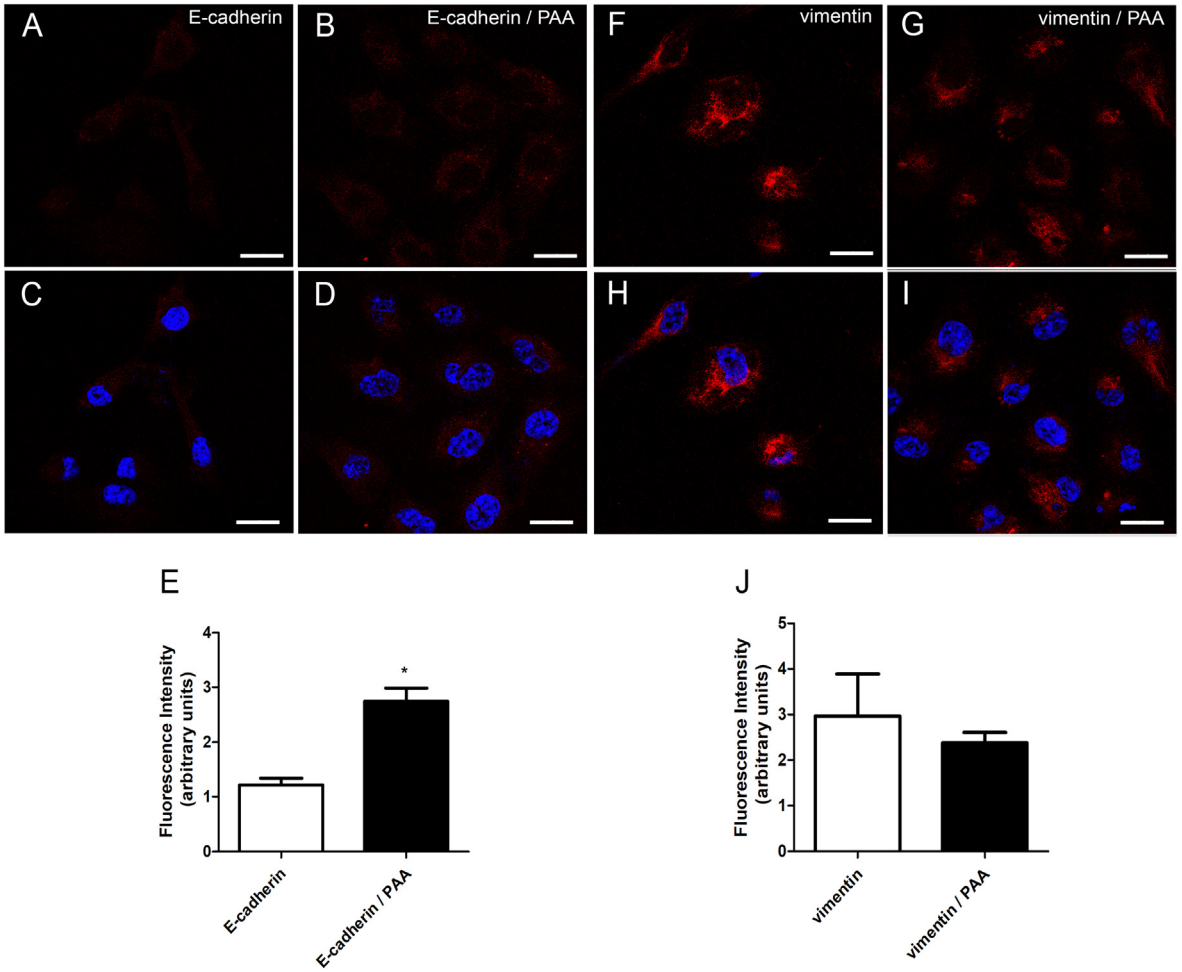

Fig. 7. Effect of PAA on E-cadherin and vimentin expression. MDA-MB-231 cells were plated onto microscope slides (5×10^4 cells/well) and then maintained in the presence or absence of 1 mM PAA for 24 h. Cells were fixed, permeabilized and the expression of E-cadherin (A–D) and vimentin (F—I) was detected by immunofluorescence. Nuclei were revealed with DAPI (blue). Bars = 20 μm. Fluorescence intensity of red-stained MDA-MB-231 cells were quantified for E-Cadherin (E) and vimentin (J).* $p < 0.0001$ vs. untreated cells. (For interpretation of the references to colour in this figure legend, the reader is referred to the web version of this article.)

transport did occur in the acidic pH range, suggesting that the putative transporter is either H^+-dependent, or that it has greater affinity for Pi in its protonated form (H_3PO_4). Similar results were found by Ito and coworkers (2005) who studied an H^+-dependent Pi transporter involved in the uptake up Pi during bone reabsorption in osteoclast-like cells [12]. In order to demonstrate the occurrence of a proton-dependent Pi transporter, the intracellular pH was quantified in the presence of phosphate. The results in Fig. 5 showed that indeed there was a reduction in the intracellular pH after adding inorganic phosphate. These results indicated that, upon addition of phosphate, protons present in the extracellular environment might be transported together with inorganic phosphate by an H^+-dependent Pi co-transporter, thus contributing to the acidification of the intracellular environment.

Bafilomycin A_1, an inhibitor of a vacuolar H^+-ATPase that may be located on the plasma membrane (responsible for the H^+-pumping to the extracellular environment), or the vacuole membrane (H^+ pumping

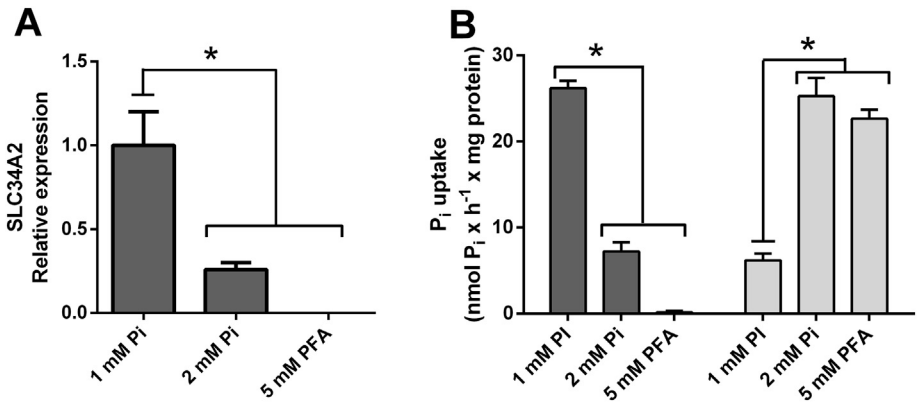

Fig. 8. Effect of high phosphate concentration and PFA in growth medium on SLC34A2 expression or Pi transport in MDA-MB-231. A) SLC34A2 expression analysis was done after pre-treatment for 24 h with 1 mM Pi (control), 2 mM Pi and 5 mM PFA. Gene expression data were normalized to an endogenous reference β-actin (ACTB). B) Intact cells (5×10^4 cells/well = 1.45 mg protein/well) were incubated for at 37 °C in a reaction mixture for H^+-dependent Pi transport (light gray) containing 116 mM choline or 116 mM NaCl for Na+-dependent Pi transport (dark gray), 5.5 mM Glucose, 5.4 KCl, 10 mM HEPES, 0.8 mM $MgCl_2$, 1 mM KH_2PO_4 and 2.5 μCi/nmol ^{32}Pi. Results are the means ± SE of at least 3 experiments, with different cell suspensions. Statistical significance was analyzed applying unpaired *t*-test.

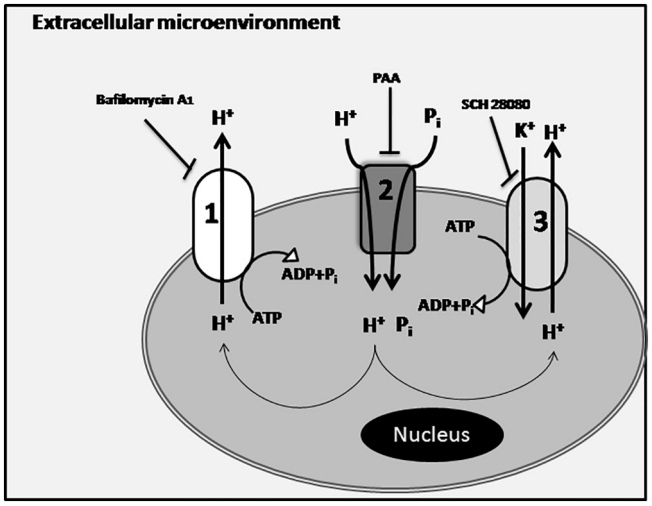

Fig. 9. Proposed mechanism for H^+-dependent Pi transporter mechanism in MDA-MB-231 cells: H^+, K^+-ATPase-Bafilomycin A1 sensitive in the plasma membrane and H^+-ATPase SCH-28080-sensitivein the plasma membrane coupled to Pi H+-dependent transporter.

to the vacuolar lumen), was able to inhibit H^+-dependent Pi transport (Fig. 4A). In addition, H^+-dependent Pi transport was inhibited by FCCP (H^+ ionophore) and SCH28080 (H^+, K^+-ATPase inhibitor) (Fig. 4A). Collectively these results indicate a role for the a vacuolar H^+-ATPase and an H^+, K^+-ATPase in the regulation of Pi, H^+ transport mechanism (Fig. 9).

We have previously shown that PFA inhibits Na^+-dependent Pi transport [26]. In the H^+-dependent Pi transport, we observed no effect of PFA. However, when looking for another inhibitor of Pi transport belonging to the same class of PFA (phosphoenolcarboxylic acids), we showed that PAA was able to inhibit the H^+-dependent Pi transport (Fig. 6A). A possible mechanistic explanation for this result is that PFA bound to phosphorus and its three sodium ions. This would increase its affinity to the sodium-dependent Pi carrier bound to the three sodium ions Pi [5]. Conversely, PAA is a compound which has phosphorus attached to oxygen and a hydroxyl at its ends; in the absence of sodium and, being structurally similar to inorganic phosphate, this molecule might be able to competitively inhibit H^+-dependent Pi transport.

Pi plays a critical role in several cell types, participating in the energy metabolism and in nucleic acid synthesis [15]. In tumor cells, phosphate is required for their rapid growth rates, in keeping with the Growth Rate Hypothesis (GRH) [15–17]. It has been shown that 3 and 5 mM Pi were able to stimulate the migration of MDA-MB-231 cells compared to normal cells grown 1 mM Pi [15,24]. Although PAA has been reported to affect DNA synthesis and cause arrest of cellular cycle, besides having antiviral activity, it is also described as a specific inhibitor of Pi transporters [12,13,32,33]. Hence we thus tested PAA on MDA-MB-231 cells, which has a higher migratory capacity than other lineages [23]. PAA was able to promote a significant reduction in cell proliferation (after 24 h), migration and adhesion (Fig. 6) in these cells without affecting their viability, thus indicating that H^+-dependent Pi transporter may be a hallmark of cancer cells. In addition, as evidenced with immunofluorescence results, MDA-MB-231 cells tend to revert from mesenchymal to epithelial features when the H^+-dependent Pi transport is inhibited in the presence of PAA (Fig. 7), consistently strengthening the observed reduction of migration capacity (Fig. 6).

Extracellular Pi in humans is maintained in a relatively narrow range, between 0.7 and 1.55 mM [3]. However, in the tumor microenvironment of mammary gland mice was identified a high concentration of Pi (approximately 2 mM) [20]. We have observed a decreased NaPi-IIb expression and Na^+-dependent Pi transport in the presence of 2 mM Pi or 5 mM PFA concomitant with an increase in H^+-dependent Pi transport (Fig. 8). This result suggested the occurrence of a compensatory mechanism for Pi transport in situations where the transport of Pi Na^+-dependent was compromised.

Amidst the paucity of studies that seek to characterize H^+-dependent Pi transport and its detailed participation in cellular mechanisms, this report described identified for the first time an H^+-dependent Pi transporter and how it could participate in several vital processes of breast tumor progression. Further studies should be directed at the structural characterization of the H^+-dependent Pi carrier. However, an added complication is the lack of information regarding the gene encoding the transporter since this has not yet been annotated. When eventually this becomes available it may be possible to confirm our hypothesis by carrying out work with the recombinant molecule which would permit the systematic and precise analysis of the parameters discussed here. Likewise, knowledge derived from the gene sequence may also enable specific interference studies of the H^+-dependent Pi transport using for example, CRISPR or the short hairpin technology.

The functional and molecular nature of the H^+-dependent Pi transporter could represent a biological advantage for tumors in the sense of endowing cells with the incorporation of extra Pi even in those conditions when the sodium-dependent Pi transport is saturated by a high extracellular Pi (approx. 2 mM). The excess Pi might be able to compensate for the energetically expensive biochemical features of tumor cells. We suggest that the dissociated tumor cells (metastatic) are able to adjust their biochemical profile as a function of changes in the microenvironment as indicated by the results shown in Fig. 6E and F. In addition, the occurrence of an H^+-dependent Pi transporter in tumor cells might represent a positive selective adaptation to the low pH in their vicinity due to lactate secretion, i.e., the transporter would favor Pi uptake even in conditions of high acidity.

Conflict of interest

The authors declare that they have no conflict of interest.

Transparency document

The Transparency document associated with this article can be found, in online version.

Acknowledgements

We would like to thank Mr. Fabiano Ferreira Esteves, Mr. Edimilson Pereira and Ms. Rosangela Rosa de Araújo for their technical assistance. This work was supported by research grants Brazilian National Council for Scientific and Technological Development (CNPq), The State of Rio de Janeiro Research Foundation (FAPERJ), and the Coordination for the Improvement of Higher Education Personnel (CAPES) supported this investigation.

We thank CENABIO (Centro Nacional de Biologia Estrutural e Bioimagem) for confocal facility.

References

[1] L. Sapio, S. Naviglio, Inorganic phosphate in the development and treatment of cancer: a Janus Bifrons? World J Clin Oncol 6 (2015) 198–201.
[2] J. Biber, N. Hernando, I. Forster, Phosphate transporters and their function, Annu. Rev. Physiol. 75 (2013) 535–550, https://doi.org/10.5306/wjco.v6.i6.198.
[3] C.E. Camalier, M. Young, G. Bober, C.M. Perella, N.H. Collburn, G.R. Beck, Elevated phosphate activates N-ras and promotes cell transformation and skin tumorigenesis, Cancer Prev. Res. 3 (2013) 359–370, https://doi.org/10.1158/1940-6207.
[4] Y.D. Bhutia, E. Babu, S. Ramachandran, S. Yang, M. Thangaraju, V. Ganapathy, SLC transporters as a novel class of tumor suppressors: identity, function and molecular mechanisms, Biochem. J. 473 (2016) 1113–1124, https://doi.org/10.1042/BJ20150751.
[5] I.C. Forster, N. Hernando, J. Biber, H. Murer, Phosphate transporters of the SLC20 and SLC34 families, Mol. Asp. Med. 34 (2013) 386–395, https://doi.org/10.1016/j.mam.2012.07.007.
[6] D.G. Miller, R.H. Edwards, A.D. Miller, Cloning of the cellular receptor for

amphotropic murine retroviruses reveals homology to that for gibbon ape leukemia virus, Proc. Natl. Acad. Sci. 91 (1994) 78–82, https://doi.org/10.1073/pnas.91.1.78.
[7] B. O'hara, S.V. Johann, H.P. Klinger, D.G. Blair, H. Rubinson, K.J. Dunn, P. Sass, S.M. Vitek, T. Robins, Characterization of a human gene conferring sensitivity to infection by gibbon ape leukemia virus, Cell Growth Differ. 3 (1990) 119–127.
[8] M.P. Kavanaugh, D. Kabat, Identification and characterization of a widely expressed phosphate transporter/retrovirus receptor family, Kidney Int. 49 (1996) 959–963.
[9] C.A. Wagner, N. Hernando, I.C. Forster, J. Biber, The SLC34 family of sodium-dependent phosphate transports, Pflugers Arch. 466 (2013) 139–153, https://doi.org/10.1007/s00424-013-1418-6.
[10] S.P. Shirazi-Beechey, J.I. Penny, J. Dyer, I.S. Wood, P.S. Tarpey, D. Scott, W. Buchan, Epithelial phosphate transport in ruminants, mechanisms and regulation, Kidney Int. 49 (1996) 992–996.
[11] K. Huber, C. Walter, B. Schroder, G. Breves, Phosphate transport in the duodenum and jejunum of goats and its adaptation by dietary phosphate and calcium, Am. J. Physiol. Regul. Integr. Comp. Physiol. 283 (2002) R296–R302, https://doi.org/10.1152/ajpregu.00760.2001.
[12] M. Ito, N. Matsuka, M. Izuka, S. Haito, Y. Sakai, R. Nakamura, R. Segawa, M. Kuwahata, H. Yamamoto, W.J. Pike, K. Miyamoto, Characterization of inorganic phosphate transport in osteoclast-like cells, Am. J. Physiol. Cell Physiol. 288 (2004) 921–931, https://doi.org/10.1152/ajpcell.00412.2004.
[13] E. Candeal, Y.A. Caldas, N. Guillèn, M. Levi, V. Sorribas, Na+-independent phosphate transport in Caco2BBE cells, Am. J. Physiol. Cell Physiol. 307 (2014) 1113–1122, https://doi.org/10.1152/ajpcell.00251.2014.
[14] J. Marks, G.J. Lee, S.P. Nadaraja, E.S. Debnam, R.J. Unwin, Experimental and regional variations in Na+ dependent and Na+-independent phosphate transport along the rat small intestine and colon, Physiol. Rep. 3 (2015) 2051–2817, https://doi.org/10.14814/phy2.12281.
[15] M.A. Lacerda-Abreu, T. Russo-Abrahão, R.Q. Monteiro, F.D. Rumjanek, J.R. Meyer-Fernandes, Inorganic phosphate transporters in cancer: functions, molecular mechanisms and possible clinical applications, Biochim. Biophys. Acta 2 (2018) 291–298, https://doi.org/10.1016/j.bbcan.2018.05.001.
[16] J.J. Elser, M.M. Kyle, M.S. Smith, J.D. Nagy, Biological stoichiometry in human cancer, PLoS One 2 (2007) e1028, https://doi.org/10.1371/journal.pone.0001028.t001.
[17] I. Kareva, Biological stoichiometry in tumor micro-environments, PLoS One 8 (2013) e51844, , https://doi.org/10.1371/journal.pone.0051844.g001.
[18] M. Stubbs, Z.M. Bhujwalla, S.G.M. Tozer, L.M. Rodrigues, R.J. Maxwell, R. Morgan, F.A. Howe, J.R. Griffiths, An assessment of 31P MRS as a method of measuring pH in rat tumours, NMR Biomed. 5 (1992) 351–359, https://doi.org/10.1002/nbm.1940050606.
[19] A. Marín-Hernández, J.C. Gallardo-Pérez, S. Rodríguez-Enríquez, R. Encalada, R. Moreno-Sánchez, E. Saavedra, Modeling cancer glycolysis, Biochim. Biophys. Acta 1807 (2011) 755–767, https://doi.org/10.1016/j.bbabio.2010.11.006.
[20] A.A. Bobko, T.D. Eubank, B. Driesschaert, I. Dhimitruka, J. Evans, R. Mohammad, E.E. Tchekneva, M.M. Dikov, V.V. Khramtsov, Interstitial inorganic phosphate as a tumor microenvironment marker for tumor progression, Sci. Rep. 7 (2017) 41233, , https://doi.org/10.1038/srep41233.
[21] D.L. Holliday, V. Speirs, Choosing the right cell line for breast cancer research, Breast Cancer Res. 13 (2011), https://doi.org/10.1186/bcr2889.
[22] C.R. Ross, K.W. Temburnikar, G.M. Wilson, K.L. Seley-Radtke, Mitotic arrest of breast cancer MDA-MB-231 cells by a halogenated thieno[3,2-d]pyrimidine, Bioorg. Med. Chem. Lett. 25 (2015) 1715–1717, https://doi.org/10.1016/j.bmcl.2015.02.071.
[23] B.N. Smith, L.J. Burton, V. Henderson, D.D. Randle, D.J. Morton, B.A. Smith, L. Taliaferro-Smith, P. Nagappan, C. Yates, M. Zayzafoon, L.W.K. Chung, V.A. Odero-Marah, Snail promotes epithelial mesenchymal transition in breast cancer cells in part via activation of nuclear ERK2, PLoS One (8) (2014) e104987, , https://doi.org/10.1371/journal.pone.0104987.
[24] Y. Lin, K.E. Mckinnon, S.W. Ha Jr., G.R. Beck, Inorganic phosphate induces cancer cell mediated angiogenesis dependent on forkhead box protein C2 (FOXC2) regulated osteopontin expression, Mol. Carcinog. 54 (2014) 926–934, https://doi.org/10.1002/mc.22153.
[25] D.R. Chen, S.Y. Chien, S.J. Kuo, Y.H. Teng, H.T. Tsai, J.H. Kuo, J.G. Chung, SLC34A2 as a novel marker for diagnosis and targeted therapy of breast cancer, Anticancer Res. 30 (2010) 4135–4140.
[26] T. Russo-Abrahão, M.A. Lacerda-Abreu, T. Gomes, D. Cosentino-Gomes, A.D. Carvalho-De-Araújo, M.F. Rodrigues, A.C.L. Oliveira, F.D. Rumjanek, R.Q. Monteiro, J.R. Meyer-Fernandes, Characterization of inorganic phosphate transport in the triple-negative breast cancer cell line, MDA-MB-231, PLoS One 13 (2018) e0191270, , https://doi.org/10.1371/journal.pone.0191270.
[27] M.M. Bradford, A rapid and sensitive method for the quantitation of microgram quantities of protein utilizing the principle of protein-dye binding, Anal. Biochem. 72 (1976) 248–254.
[28] T. Russo-Abrahão, M. Alves-Bezerra, D. Majerowicz, A.L. Freitas-Mesquita, C.F. Dick, K.C. Gondim, J.R. Meyer-Fernandes, Transport of inorganic phosphate in *Leishmania infantum* and compensatory regulation at low inorganic phosphate concentration, Biochim. Biophys. Acta 1830 (2013) 2683–2689, https://doi.org/10.1016/j. bbagen.2012.11.017.
[29] L.L. Liu, H. Zhao, T.F. Ma, F. Ge, C.S. Chen, Y.P. Zhang, Identification of valid reference genes for the normalization of RT-qPCR expression studies in human breast cancer cell lines treated with and without transient transfection, PLoS One 10 (2015) e0117058, , https://doi.org/10.1371/journal.pone. 0117058.
[30] L. Wang, X. Zhou, T. Zhou, D. Ma, S. Chen, X. Zhi, L. Yin, Z. Shao, Z. Ou, P. Zhou, Ecto-5′-nucleotidase promotes invasion, migration and adhesion of human breast cancer cells, J. Cancer Res. Clin. Oncol. 134 (2008) 365–372, https://doi.org/10.1007/s00432-007-0292-z.
[31] J.A. Thomas, R.N. Buchsbaum, A. Zimniak, E. Racker, Intracellular pH measurements in Ehrlich ascites tumor cells utilizing spectroscopic probes generated in situ, Biochemistry 18 (1979) 2210–2218.
[32] O. Nyormoi, D.A. Thorley-Lawson, J. Elkington, J.L. Strominger, Differential effect of phosphonoacetic acid on the expression of Epstein-Barr viral antigens and virus production, Proc. Natl. Acad. Sci. 73 (5) (1976) 1745–1748.
[33] M. Loghman-Adham, Use of phosphonocarboxylic acids as inhibitors of sodium-phosphate cotransport, Gen. Pharmacol. 27 (2) (1996) 305–312, https://doi.org/10.1016/0306-3623(95)02017-9.